

Spatial symmetry breaking by non-local Kerr-lensing in mode-locked lasers

Idan Parshani¹, Leon Bello^{1,2}, Mallachi-Elia Meller¹, Avi Pe'er^{1*}

¹ Department of Physics and BINA Institute of Nanotechnology,
Bar-Ilan University, Ramat-Gan 52900, Israel and

² Department of Electrical and Computer Engineering, Princeton University, Princeton, NJ

(Dated: November 24, 2021)

Kerr-lens mode-locking (KLM) is the work-horse mechanism for generation of ultrashort pulses, where a non-linear lens forms an effective ultrafast saturable absorber within the laser cavity. According to standard theory, the pulse in the cavity is a soliton, with a temporal profile and power determined by the non-linearity to exactly counteract diffraction and dispersion, resulting in pulses, whose power and shape are fixed across a wide range of pump powers. We show numerically and demonstrate experimentally that the non-local effect of the Kerr lens in a linear cavity allows the laser to deviate from the soliton model by breaking the spatial symmetry in the cavity between the forward and backward halves of the round-trip, and hence to extract more power in a single pulse, while maintaining stable cavity propagation. We confirm this prediction experimentally in a mode-locked Ti:Sapphire laser with a quantitative agreement to the simulation results. Our numerical tool opens new avenues to optimization and enhancement of the mode-locking performance based on direct examination of the Kerr medium and the spatio-temporal dynamics within it, which is difficult (or even impossible) to observe experimentally.

Keywords: Lasers, Mode-Locking, Solitons

I. INTRODUCTION

Kerr-lens mode-locking (KLM) is a passive mode-locking technique for producing ultra-short pulses [1–3]. It utilizes a third-order (Kerr) non-linear lensing effect to create an effective ultra-fast saturable absorber, which acts to diffract out low-power CW and stabilize pulses with higher peak power, by focusing them through an effective hard-aperture in the cavity, thereby reducing the loss for pulses [4–6]. According to standard theory, these stable Kerr pulses are solitons, and are only stable for precisely the intra-cavity pulse power that generates the Kerr-lens of the required focal length to counteract the diffraction loss of the cavity [1, 6–12], as illustrated in Fig. 1.

The spatial profile of the laser beam across the cavity is normally dictated by cavity-stability analysis, requiring the cavity mode to repeat after every round trip. In a linear cavity, the propagation in the forward and backward directions through the cavity is inherently symmetric, due to the inversion symmetry of all optical elements and the exact inversion of the phase-front on the end mirrors [13]. The standard model of KLM in a linear cavity assumes this symmetry also for the nonlinear Kerr-lens that stabilizes the cavity mode for pulsed operation (see figure 1), which requires a specific peak-power and pulse shape to form the specific focal length of the Kerr lens, and hence - a soliton. Once formed, the pulse energy is fixed, and any additional power in the cavity (due to elevated pumping, for example) can-

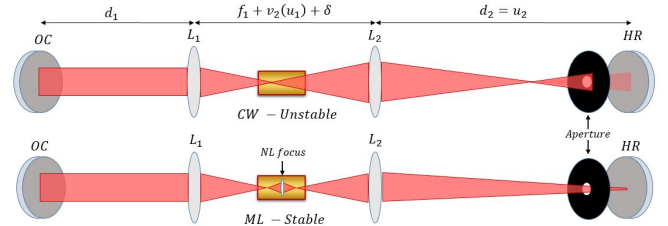


Figure 1. The soliton model of KLM: The Kerr effect in the gain medium (red) acts to focus the beam inside the cavity, mitigating diffraction losses for pulses with high peak power. **(top)** Linear beam propagation inside the cavity **(bottom)** Beam propagation with the Kerr lens for pulsed operation. d_{12} are the distances in the free propagation arms of the cavity, between the end mirrors (denoted by **OC** and **HR**) and the focusing elements (denoted L_{12}) with focal lengths f_{12} , respectively. The total distance between the focusing elements deviates from the imaging condition by δ , and also quantifies the cavity stability. The aperture does not need to physically exist, but is there to illustrate the role of the diffraction losses in the cavity.

not increase the circulating energy, but rather be lost to amplified-spontaneous emission (ASE), or lead to additional continuous-wave (CW) lasing or form additional pulses in the oscillation [14, 15].

Since the light in a linear cavity interacts with the Kerr medium twice, the nonlinear effect is *non-local*. We show quite generally, that the pulses in a linear cavity do not follow the expected soliton picture, which indicates a major difference between KLM in a linear cavity and in a ring cavity [16, 17]. The non-local Kerr-lens breaks the spatial symmetry between the forward

* Correspondence email address: avi.pe'er@biu.ac.il

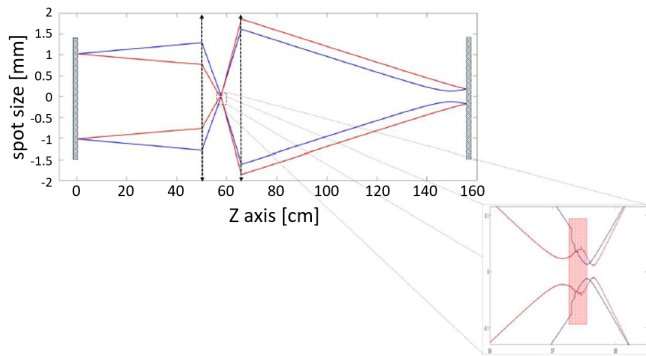


Figure 2. Symmetry-breaking between the forward and backwards halves of the cavity round trip (simulation): The oscillator breaks the propagation symmetry in order to employ higher pulse power and energy. The figure shows the numerically simulated beam waist during the entire round-trip in the cavity, where the forward half (blue) is different from the backwards half (red), exhibiting different focusing power through each. **Inset:** zoom-in on the beam profile within the nonlinear Kerr medium

and backwards halves of the cavity round-trips. Accordingly, the pulse generates a stronger non-linear lens in the forward half of the round trip, which leads to over-focusing in the forward direction at the expense of a weaker one in the backwards half (due to a larger beam area and lower intensity), as outlined in figure 2. Consequently, only after a complete round-trip will the pulse repeat its shape and spatial profile, but not between the halves of the round-trip.

We identified this effect theoretically and then confirmed it in an experiment with a home-brewed KLM Ti:Sapphire cavity. The theoretical prediction originated from a numerical simulation tool that we developed to observe the complete spatio-temporal dynamics and evolution of a pulse in the cavity, under rather general assumptions. Previously, this tool served us for demonstrating the dynamical loss mechanism in KLM [18].

The Kerr nonlinearity is known to break the symmetry between oscillation modes that are originally symmetric. For example, the symmetry between the two polarizations in micro-ring cavities is broken by Kerr [19], and the clockwise and counter-clockwise oscillations modes cannot coexist in ring fibers with Kerr nonlinearity [19–21]. Here however, we show that a non-local Kerr-lens breaks the symmetry even within a single mode of oscillation.

Our simulation offers a powerful utility for laser physics and engineering with KLM, since it exposes the complete spatio-temporal propagation dynamics of the pulse *within the nonlinear medium*, where experimental probes do not exist. It simulates the evolution of the ultrafast laser oscillation on both fast and slow time

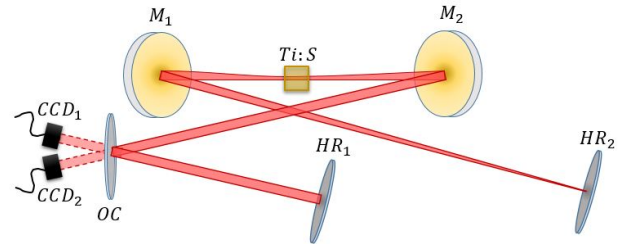


Figure 3. Experimental configuration: We employ a standard X-folded four-mirror cavity. **M1(2)** Spherical mirrors with $f = 75\text{mm}$. **HR1(2)** are the highly reflecting end mirrors (flat). **OC** is the output coupler used to probe the beam twice in each round-trip. A pair of BK7 prisms is deployed to compensate for intra-cavity dispersion (not shown). The gain medium (and Kerr medium) is a 3mm long Ti:Sapphire crystal (0.25% doped), pumped by a 4W-6W laser at 532nm (Verdi V18 by Coherent). The generated pulses have a repetition rate of 67MHz and a duration of roughly 50fs.

scales. The fast one captures the dynamics within a single round-trip, inflicted by the Kerr lens on the temporal field envelope of the pulse and the temporal beam profile (the time dependent waist and phase front). The slow one represents the evolution from one round-trip to the next, simulating the convergence towards steady state due to different propagation effects. This provides the critical capability to test and optimise novel designs and concepts of KLM prior to implementation, which rely primarily on intuition.

The simulation assumes a Gaussian beam profile and employs a time dependent ABCD matrix $M_n(t)$ to represent the cavity propagation of round-trip n for every time-bin t of the pulse. Repeating the propagation from one round-trip to the next, while updating the ABCD matrix according to the laser evolution allows to observe the complete cavity dynamics from initiation to steady state oscillation. Although other numerical analyses of KLM have used the temporal ABCD formalism before [2, 14, 22–27], they all assumed a local Kerr interaction and were all aimed directly at finding the steady state oscillation, not at the dynamical cavity evolution.

The ‘results’ section below details the experimental observations of symmetry breaking within the cavity for output power, beam profile and laser-threshold, and highlights the quantitative agreement with the numerical predictions. A detailed review of the numerical simulation is given in the ‘methods’.

II. RESULTS

In our experiment, we employ a standard Ti:Sapphire oscillator in an X-folded cavity [28, 29], as shown in fig-

ure 3. In order to observe the intra-cavity beam in both forward and backwards directions, a planar output coupler (reflectivity $R = 0.98$) folds the cavity configuration near one of the focusing mirrors and couples out a fraction of the intra-cavity beam in both directions to be imaged on a CCD camera. The results show quantitative agreement to the numerical simulation. We show that this symmetry breaking allows the pulse power to increase with the pump power, as illustrated in figures 4,5 allowing the laser to improve the light efficiency contrary to the soliton model.

The distance between the mirrors is offset by δ from a perfect telescope, corresponding to different stable or unstable ray configurations, with our cavity operated slightly outside the stability zone, which induces diffraction losses for CW operation. For high peak-intensity pulses, the Kerr-lens counteracts the diffraction losses and pushes the cavity back into spatial stability, inducing an effective fast saturable absorber, whose strength can be controlled by adjusting δ , i.e. moving further away from the stability zone.

Our analysis (figure 2) shows a broad regime outside the stability zone and above the oscillation threshold, where the laser changes its temporal profile such that it induces different optical powers in the Kerr medium through the two otherwise identical halves of the round-trip. This asymmetry shows a quantifiable signature - the beam waist at the same location changes considerably between the forward and backwards direction. All of these findings were first predicted by the numerical simulation and only later verified experimentally.

Interestingly, the simulation shows that the maximum output power (at a fixed pump) is achieved when the crystal is offset from the focal point of the short arm's lens by $\sim 1\text{mm}$ in the direction of the short arm of the cavity [24]. This optimal offset directly contradicts the soliton-mode model, which predicts an optimal lens position *in the opposite direction*. Experimental measurement of the pump threshold for ML as for different crystal positions shows a clear optimum. Although the experimental uncertainty in the exact offset position of the crystal ($\sim 1\text{mm}$) prevents unequivocal verification of the optimum location, the width of the optimum agrees well with the simulation.

Figure 4 shows the ratio between the measured widths (FWHM) of the forward and backward beams on the CCD, while scanning the pump power. Clearly the beam size asymmetry increases linearly with the pump, in good agreement with the numerical predictions. The corresponding measurement of the total output power of the laser (figure 5) also shows a linear increase with pump power, violating the soliton assumption.

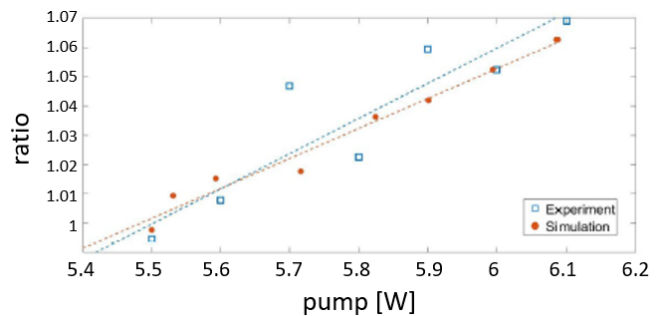


Figure 4. Ratio of intra-cavity beam width between the forward and backwards directions. Blue - measured, as captured on the two cameras (CCD1 and CCD2). Red - numerical simulation. The asymmetry ratio increases with the pump power in accordance with the increase of the total output power and with the deviation from the soliton assumption.

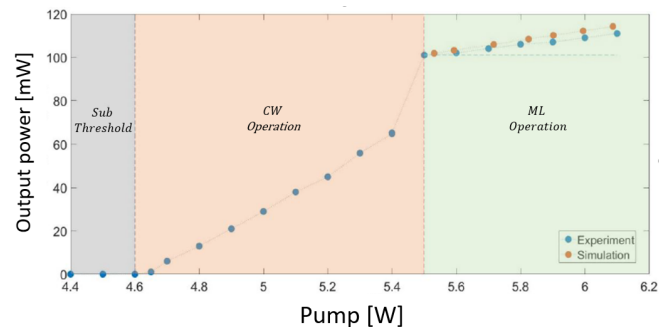


Figure 5. Output power as function of input pump power, measured experimentally (blue). We observe three regions. (1) Below the lasing threshold, where the output power is low. (2) Above the CW lasing threshold, where the output power varies linearly with the pump. (3) Above the ML lasing threshold, where a linear increase is still observed, but with a lower slope, deviating from the soliton assumption. For comparison, we also show the simulation predicted output power (red, fitted only for the ML threshold), which predicts nearly the same power slope as the measurement.

III. CONCLUSIONS

In summary, we uncovered through numerical analysis and verified experimentally an effect of symmetry-breaking in KLM lasers when the Kerr-lens effect is non-local. Namely, the spatial symmetry between identical parts of the cavity can be broken. When the Kerr lens interaction occurs more than once during the round-trip, as the case in a linear cavity between the forward and backwards propagation. This symmetry breaking allows the laser to enhance its power efficiency beyond the soliton solution [1], and renders the linear KLM cavity inherently different from the ring cavity.

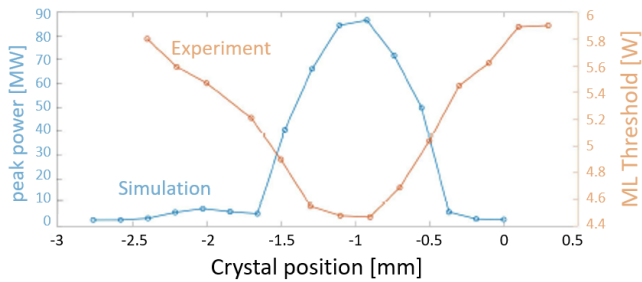


Figure 6. Optimal crystal position for ML efficiency - experiment and numerical simulation. **Blue** - the numerically calculated ML peak-power, and orange - the experimental ML threshold, as a function of the crystal offset from the focal point of the short arm’s lens towards the long arm of the cavity (see figure 1 for definition). Interestingly, the optimal crystal position is offset *in the opposite direction* from the conventional expectation assuming a soliton mode.

From the engineering aspect, the numerical simulation tool is a powerful utility for KLM laser design, since it directly visualizes the spatio-temporal propagation of the pulse *within the nonlinear medium*, where experimental observation can only be indirect. This allows to systematically evaluate and optimize new concepts of KLM [15] prior to implementation.

IV. METHODS

We hereby review the concept and operation procedure of the numerical simulation. A thorough discussion of the simulation details and additional verification tests are deferred to a later publication.

We calculate the dynamical evolution of the pulse in the cavity in both space and time, and consider its dynamical properties as well as its final steady-state. We focus on the hard-aperture KLM regime, where diffraction losses are the dominant effect.

We approximate the spatial mode of the laser to be a single transverse Gaussian TEM_{00} mode, whose waist is intensity-dependent and varies in time due to the Kerr-lens (which is time-dependent). This assumption of a single spatial-mode is legitimate for KLM oscillators in free-space, which are strongly driven by the hard aperture towards a single spatial mode [29]. Specifically, higher transverse modes are not able to properly induce the Kerr lens and are strongly suppressed by the diffraction losses. Under this Gaussian approximation, the spatial amplitude profile of the beam during the n -th round trip is fully represented by a time-dependent complex beam parameter q_n . The beam profile for the subsequent round trip is $q_{n+1}(t) = (Aq_n(t) + B) / (Cq_n(t) + D)$, which follows the standard cavity propagation using ABCD analy-

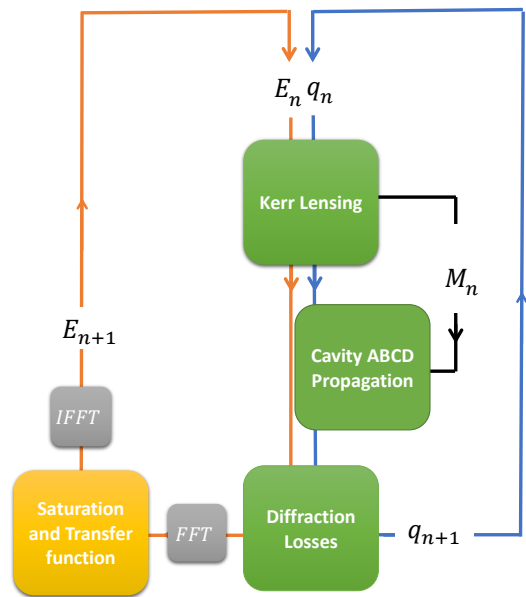


Figure 7. Flow diagram of the simulation. In each round-trip n , the simulation maintains two vectors - E_n , the instantaneous field envelope of the pulse and q_n , the instantaneous complex beam parameter. Using these two vectors, we can calculate the instantaneous non-linear lens based on the instantaneous intensity distribution, which can then be combined into the complete ABCD matrix M_n of the cavity round-trip, which allows to propagate the beam and calculate the new complex beam parameter q_{n+1} . The instantaneous diffraction losses during the round-trip can then be calculated based on the new complex beam parameter and the assumed aperture function. Finally, gain saturation, finite gain bandwidth and cavity dispersion are applied in frequency domain to the field, providing the field envelope E_{n+1} for the next round-trip.

sis [13]. Note however that here the ABCD matrix of the round-trip is time dependent since it includes the intensity-dependent Kerr-lens, which varies according to the temporal intensity of the intra-cavity pulse, as well as from one round-trip to the next (due to the gain evolution).

We calculate therefore the complex field envelope on two time-scales, a “slow” time-scale, which accounts for the variations from one round-trip to the next, and a “fast” time-scale, which measures the intra-cavity evolution within the round-trip due to the Kerr-lens effect. Our simulation makes no explicit definition of the carrier frequency, which is completely arbitrary, and simulates only the complex temporal envelope of the pulse. The simulation flow is outlined in figure 7, applying dispersion and linear gain/loss in frequency-domain, while saturation and the Kerr-effect are applied in the time-domain, where they are more naturally described.

The simulation accepts several parameters that re-

flect the known (or measured) properties of the laser in question - the nonlinear Kerr coefficient, the net dispersion of the cavity, the gain bandwidth (assuming Gaussian gain spectrum), the small-signal gain and loss, gain saturation parameter, gain spatial profile (pump-mode width at the gain medium) and the loss function. The aperture can be located everywhere in the cavity, for example near one of the end mirrors. In our experimental setup the diffraction losses caused by the mismatch between the cavity spatial mode and the pump mode in the gain medium ("virtual" hard-aperture). Therefore the spatial width of the aperture matched to the measured pump spot size in the crystal.

The simulation maintains and updates two major vectors: the pulse field envelope $E_n(t)$ and the complex beam parameter $q_n(t)$ in each round trip n . Initially, the field envelope and complex beam parameter are taken as low-intensity random noise ($E_0(t), q_0(t)$), that represent the spontaneous emission seed. They are then propagated repeatedly through four modules (see figure 7), simulating the important steps in the pulse evolution: Kerr lensing and self-phase modulation, cavity propagation, diffraction losses (hard aperture), gain and dispersion. This process is repeated until the intra-cavity pulse profile stabilizes. The simulation parameters were matched to our experimental apparatus like the distance between the mirrors and the lenses and the thickness of the gain medium, but clearly the parameters can be changed to match other systems as well.

The cavity propagation employs a time-dependent ABCD matrix $M_n(t)$ that incorporates the non-linear lens along with the other linear optical elements in the cavity. The focal power of the non-linear Kerr-lens is calculated according to $1/f_n(t) = 8n_2dP_n(t)^2/\pi w_n(t)^4$, based on the intra-cavity power $P_n(t)$, the beam width $w_n(t)$ (from the complex beam parameter $q_n(t)$), the non-linear refractive index n_2 and the thickness of the Kerr medium d .

Finally, we calculate the total gain and time-dependent loss of the round-trip. This is divided into two components - the fast, time-dependent losses due to the hard-aperture, and the slow gain saturation, dispersion and linear losses, which are computed in frequency domain, where they can be calculated efficiently with a simple transfer function of the spectral gain and dispersion profile. To account for gain saturation, we calculate the mean power over the roundtrip \bar{P}_n and compute the gain saturation $g_n = 1/(1 + \bar{P}_n/P_{ss})$, where $P_{ss} = 2.6\text{W}$ is the saturation power, calculated using the transition cross section and the upper-state lifetime of Ti:Sapphire [30]. The gain dynamics is assumed to be slow compared to the pulse time scale, which is well validated for femtosecond pulses in a CW-pumped Ti:Sapphire oscillator. Specifically, our simulation incorporates gain depletion by each pulse proportional to the total pulse energy due to the laser-pump coupling and assumes that gain replenish occurs slowly between cavity round-trips (neglecting the dynamics within the ultrashort femtosecond pulse itself).

-
- [1] J. Herrmann, *J. Opt. Soc. Am. B* (1994).
 - [2] P. F. C. T. Brabec, Ch. Spielmann and F. Krausz, *Optics Letters* **17** (1992).
 - [3] T. Brabec, A. J. Schmidt, P. F. Curley, C. Spielmann, and E. Wintner, *J. Opt. Soc. Am. B* **10** (1993).
 - [4] F. X. Kurtner, J. A. d. Au, and U. Keller, *IEEE Journal of Selected Topics in Quantum Electronics* **4**, 159 (1998), publisher: Institute of Electrical and Electronics Engineers (IEEE).
 - [5] A. B. Matsko, A. A. Savchenkov, W. Liang, V. S. Ilchenko, D. Seidel, and L. Maleki, *Optics Letters* **36**, 2845 (2011), publisher: The Optical Society.
 - [6] H. A. Haus, *IEEE Journal on Selected Topics in Quantum Electronics* **6** (2000).
 - [7] H. A. Haus, *J. Appl. Phys.* **46** (1975).
 - [8] E. P. Ippen, *Applied Physics B Laser and Optics* **58**, 159 (1994), publisher: Springer Science and Business Media LLC.
 - [9] F. Kartner, I. Jung, and U. Keller, *IEEE Journal of Selected Topics in Quantum Electronics* **2**, 540 (1996).
 - [10] H. Haus, D. Jones, E. Ippen, and W. Wong, *Journal of Lightwave Technology* **14**, 622 (1996).
 - [11] I. D. Jung, F. X. Kärtner, L. R. Brovelli, M. Kamp, and U. Keller, *Opt. Lett.* **20**, 1892 (1995).
 - [12] X. Liu, D. Popa, and N. Akhmediev, *Phys. Rev. Lett.* **123**, 093901 (2019).
 - [13] A. E. Siegman (University Science Books, 1986) section: 20.
 - [14] S. Coen, H. G. Randle, T. Sylvestre, and M. Erkintalo, *Optics Letters* **38**, 37 (2012), publisher: The Optical Society.
 - [15] M. E. Meller, S. Yefet, and A. Pe'er, *IEEE Journal of Quantum Electronics* **53** (2017), 10.1109/jqe.2017.2670544.
 - [16] A. Dunlop, W. Firth, and E. Wright, *Optics Communications* **138**, 211 (1997).
 - [17] P. K. A. W. C. J. Chen and C. R. Menyuk, *Optics Letters* **20** (1995).
 - [18] I. Parshani, L. Bello, M.-E. Meller, and A. Pe'er, *Optics Letters* **46**, 1530 (2021).
 - [19] G. Xu, A. U. Nielsen, B. Garbin, L. Hill, G.-L. Oppo, J. Fatome, S. G. Murdoch, S. Coen, and M. Erkintalo, *Nature Communications* **12**, 4023 (2021).
 - [20] L. Del Bino, J. M. Silver, S. L. Stebbings, and P. Del'Haye, *Scientific Reports* **7**, 43142 (2017).
 - [21] I. Hendry, W. Chen, Y. Wang, B. Garbin, J. Javaloyes, G.-L. Oppo, S. Coen, S. G. Murdoch, and M. Erkintalo, *Physical Review A* **97**, 053834 (2018).

- [22] V. Magni, G. Cerullo, and S. De Silvestri, Optics Communications **96**, 348 (1993).
- [23] F. Salin, M. Piché, and J. Squier, Optics Letters **16**, 1674 (1991), publisher: The Optical Society.
- [24] Yoo, Byung Duk, Lee, Byoung Chul, R. Y. Choo, Y. H. Cha, Y. Jong Hoon, and Y. W. Lee, **46**, 1131 (2005).
- [25] D.-G. Juang, Y.-C. Chen, S.-H. Hsu, K.-H. Lin, and W.-F. Hsieh, J. Opt. Soc. Am. B **14**, 2116 (1997).
- [26] G. Cerullo, S. D. Silvestri, and V. Magni, Opt. Lett. **19**, 1040 (1994).
- [27] B. Henrich and R. Beigang, Optics Communications **135**, 300 (1997).
- [28] S. Yefet and A. Pe'er, Optics Express **21**, 19040 (2013), publisher: The Optical Society.
- [29] S. Yefet and A. Pe'er, Applied Sciences **3**, 694 (2013).
- [30] To calculate the saturation power use the rp-photonics calculator in https://www.rp-photonics.com/saturation_power.html.